

Sparse blind deconvolution of seismic data via spectral projected-gradient

Entao Liu^{*1}, Naveed Iqbal^{†2}, James H. McClellan^{‡1}, and Abdullatif A. Al-Shuhail^{§2}

¹Center for Energy and Geo Processing (CeGP) at Georgia Tech and KFUPM, Atlanta, GA, USA, 30308

²Center for Energy and Geo Processing (CeGP) at Georgia Tech and KFUPM, Dhahran, Saudi Arabia, 31261

November 16, 2016

Abstract

We present an efficient numerical scheme for seismic blind deconvolution in a multichannel scenario. The method is iterative with two steps: wavelet estimation across all channels and refinement of the reflectivity estimate simultaneously in all channels using sparse deconvolution. The reflectivity update step is formulated as a basis pursuit denoising problem that is solved with the spectral projected-gradient algorithm which is known to be a very fast computational method for obtaining the sparse solution of this problem. Wavelet re-estimation has a closed form solution when performed in the frequency domain by finding the minimum energy wavelet common to all channels. In tests with both synthetic and real data, this new method yields high quality comparable to existing methods with significantly less computational effort.

1 Introduction

Seismic deconvolution is a standard procedure in seismic data processing to estimate the wavelet and then remove its effect as much as possible [Rietsch, 1997], which also attenuates reverberations and short-period multiples. Seismic deconvolution is an important step in the pre- and post-stack seismic processing workflow, because it produces a more interpretable seismic section.

^{*}entao.liu@ece.gatech.edu

[†]naveediqbal@kfupm.edu.sa

[‡]jim.mcclellan@ece.gatech.edu

[§]ashuhail@kfupm.edu.sa

Deconvolution techniques are widely adopted in seismic exploration [Tria et al., 2007, van der Bann and Pham, 2008] and seismology applications [Bostock and Sacchi, 1997, Bostock, 2004, Behm and Shekar, 2014]. A common challenge in seismic deconvolution is *blind deconvolution* where the blurring kernel, i.e., the seismic source wavelet, is unknown [Ulrych et al., 1995].

In a seismic survey, the convolution of the source wavelet with the subsurface reflectivity series is recorded as seismic traces at receivers. In a multichannel scenario [Xu et al., 1995, Kaaresen and Taxt, 1998, Ram et al., 2010], the seismic traces are typically modeled as convolutions of the same waveform with multiple reflectivity models. Early work on seismic blind deconvolution depended on two major assumptions: the impulse response of the earth is a white sequence and the source wavelet is minimum phase. In order to overcome these two limitations, homomorphic deconvolution [Otis and Smith, 1977, Herrera and van der Bann, 2012] and minimum entropy deconvolution (MED) [Wiggins, 1978] were developed. In seismic applications, conventional multichannel methods cannot be applied directly. The major cause is the great similarity between neighboring reflectivity sequences, which makes the problem either numerically sensitive or, at worst, ill-posed and impossible to solve [Nose-Filho et al., 2016].

In order to tackle this issue, a sparsity promoting regularization approach has been proposed [Gholami and Sacchi, 2012]. The prevailing methods, called sparse multichannel blind deconvolution (SMBD) [Kazemi and Sacchi, 2014] and its variant modified SMBD [Kazemi et al., 2016], perform well for both synthetic and real data sets. However, their computational complexity is proportional to the square of the number of traces which constrains them from being applied to large data sets directly, although a common solution of this issue is to apply these algorithms on data patches. The other alternative is a series of variants of the deconvolution filtering design method, such as the widely adopted predictive deconvolution [Yilmaz, 2001], and the fast algorithm for sparse multichannel blind deconvolution (F-SMBD) [Nose-Filho et al., 2016]. These approaches yield a deconvolution filter according to some criteria such as least-squares, or the smoothed ℓ_1 norm of the deconvolved signal. Compared with the SMBD method, their computation time is much lower. However, the short filter length limits F-SMBD in producing a wide band spiky deconvolution result, or increases the noise at the output of a Wiener deconvolution filter.

In this work we propose an efficient blind deconvolution scheme based on basis pursuit type of optimization and wavelet estimation which takes advantages of the multichannel nature of a seismic section and band-limited characteristics of the seismic source wavelet. The basis pursuit here is implemented by spectral projected-gradient (SPG) algorithm, which is fast, suitable for large scale problems, and applicable for complex values. But even more important, using SPG mitigates the tricky issue of choosing a good regularization parameter, using instead a constraint with physical meaning. Currently, in most of the blind deconvolution methods, such as SMBD and modified SMBD, the optimal parameter is determined by L-curve or general cross-validation (GCV) method. In both approaches, the determination of a good parameter λ , which controls the balance between sparsity of the reflectivity and loyalty to the data, actually re-

quires multiple realizations of the numerical experiments. Tests of the proposed algorithm with both synthetic and real data illustrates that this new approach gives fast and high quality deconvolution results (in the sense of quality metrics and computing time). In order to show the effectiveness of our method we have used recently proposed methods, SMBD and F-SMBD as reference techniques.

2 SMBD and F-SMBD

A recorded seismic trace can be modeled as the output of a linear system [Robinson and Treitel, 1980] in which a seismic source wavelet is convolved with the earth's impulse response. In particular, the j -th received seismic trace can be written as

$$d_j[n] = w[n] * r_j[n] + z_j[n] = \sum_k w[n-k]r_j[k] + z_j[n], \quad \text{for } n = 1, \dots, N, \quad (1)$$

where N is the number of received data samples per trace. In matrix-vector form

$$\mathbf{d}_j = \mathbf{W}\mathbf{r}_j + \mathbf{z}_j, \quad \text{for } j = 1, \dots, J, \quad (2)$$

where J is the number of channels, \mathbf{W} is an $N \times N$ convolution matrix formed from $w[n]$, \mathbf{r}_j the vector of reflectivities for the j -th channel, \mathbf{d}_j the received data vector, and \mathbf{z}_j a noise vector. Elements of the convolutional model are depicted in Figure 1.

In this section, we revisit the SMBD and F-SMBD methods which will serve as benchmarks for the comparison with our proposed method. The z -transform of (1) gives

$$D_j(z) = W(z)R_j(z) + Z_j(z). \quad (3)$$

By considering (3) for a pair of traces, we can eliminate the wavelet term $W(z)$ and obtain the following system of equations

$$D_p(z)R_q(z) - D_q(z)R_p(z) = Z_p(z)R_q(z) - Z_q(z)R_p(z), \quad \text{for } p \neq q. \quad (4)$$

which is referred to as Euclid deconvolution [Rietsch, 1997, Xu et al., 1995]. It is convenient to write (4) in matrix form:

$$\mathbf{D}_p\mathbf{r}_q - \mathbf{D}_q\mathbf{r}_p = \mathbf{Z}_p\mathbf{r}_q - \mathbf{Z}_q\mathbf{r}_p, \quad (5)$$

where $\mathbf{D}_{p(q)}$ and $\mathbf{Z}_{p(q)}$ are $N \times N$ convolution matrices formed from the received data and the noise in channels p and q . Combining all instances of (5) into one equation, we have

$$\mathbf{A}\mathbf{x} = \mathbf{e}, \quad (6)$$

where \mathbf{x} is a JN -element vector of concatenated reflectivity series for all J channels

$$\mathbf{x} = [\mathbf{r}_1^T, \mathbf{r}_2^T, \dots, \mathbf{r}_J^T]^T, \quad (7)$$

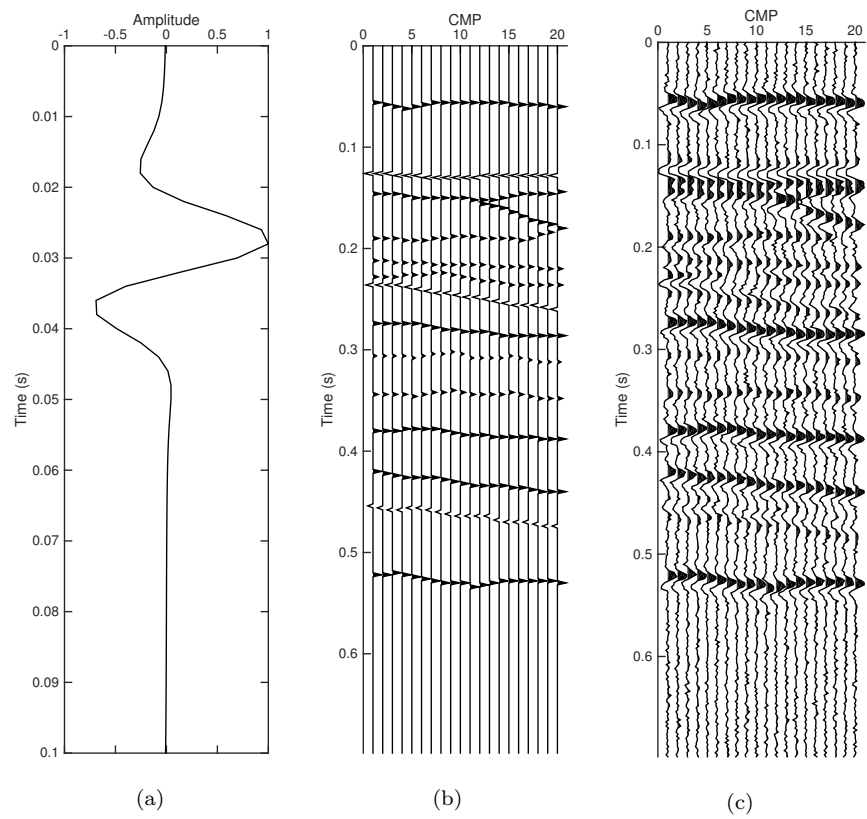


Figure 1: Convolutional model, (a) short-duration wavelet, (b) true reflectivity, (c) received traces with additive noise (SNR = 10 dB).

\mathbf{A} is a $\frac{1}{2}(J-1)JN \times JN$ matrix, and the vector \mathbf{e} is also a $\frac{1}{2}(J-1)JN$ -element vector formed by concatenating all the right-hand side vectors in (5). If the convolution model is a perfect fit to the data, then the noise terms \mathbf{z}_j in (2) are zero and $\|\mathbf{e}\| = 0$. Conversely, if $\|\mathbf{e}\| = 0$ and all $\|\mathbf{r}_j\| \neq 0$, then all the noise terms \mathbf{z}_j in (2) must be zero, which implies that the convolution model is a perfect fit to the data.

In general, the vector \mathbf{e} is an error to be minimized [Kazemi and Sacchi, 2014]. In SMBD, the energy $\|\mathbf{e}\|_2^2$ is minimized while observing a regularization constraint, i.e.,

$$\hat{\mathbf{x}} = \underset{\mathbf{x}}{\operatorname{argmin}} \left\{ \frac{1}{2} \|\mathbf{A}\mathbf{x}\|_2^2 + \lambda \mathcal{R}_\epsilon(\mathbf{x}) \right\}, \quad \text{subject to } \mathbf{x}^T \mathbf{x} = 1. \quad (8)$$

The constraint $\mathbf{x}^T \mathbf{x} = 1$ rules out a trivial solution in (8). To make the optimization easier, the regularization term is defined with a differentiable smoothed ℓ_1 -like norm

$$\mathcal{R}_\epsilon(\mathbf{x}) = \sum_n \left(\sqrt{(x[n])^2 + \epsilon^2} - \epsilon \right) \quad (9)$$

which is used to promote sparsity of the output $\hat{\mathbf{x}}$. Small values of the parameter ϵ generate a mixed norm that behaves like the ℓ_1 norm when $|x[n]| < \epsilon$, i.e., $\mathcal{R}_\epsilon(\mathbf{x}) \approx \|\mathbf{x}\|_1$.

Recently, a modified SMBD has been proposed [Kazemi et al., 2016] in which the J reflectivity series and the source wavelet are estimated via

$$\{\hat{\mathbf{x}}, \hat{\mathbf{w}}\} = \underset{\mathbf{x}, \mathbf{w}}{\operatorname{argmin}} \left\{ \|\mathbf{A}\mathbf{x}\|_2^2 + \lambda_x \|\mathbf{x}\|_1 + \lambda_n \|\mathbf{W}\mathbf{x} - \mathbf{d}\|_2^2 + \lambda_w \|\mathbf{w}\|_2^2 \right\}, \quad (10)$$

which is solved according to the following strategy.

“...by an alternating minimization technique. By fixing the source wavelet the problem can be solved for the reflectivity using any L_2 - L_1 solvers. By fixing the reflectivity, using the updated version of it, the estimation of the source wavelet can be cast as an L_2 - L_2 problem which has a closed form solution. We repeat the alternating process till convergence. There are three regularization parameters one needs to choose.”

The F-SMBD method devises a single deconvolution filter $v[n]$ that operates on all the traces $y_j[n] = d_j[n] * v[n] = \sum_k v[k]d_j[n-k]$ by minimizing the sum of the smoothed ℓ_1 norms of the deconvolved traces $y_j[n]$. Thus the following optimization problem is solved for the vector of P filter coefficients $\mathbf{v} = [v[1], \dots, v[P]]^T$,

$$\hat{\mathbf{v}} = \underset{\mathbf{v}}{\operatorname{argmin}} \mathcal{L}(\mathbf{v}) = \underset{\mathbf{v}}{\operatorname{argmin}} \sum_j \mathcal{R}_\epsilon(\mathbf{y}_j), \quad \text{subject to } \mathbf{v}^T \mathbf{v} = 1, \quad (11)$$

where the sparsity-promoting norm \mathcal{R}_ϵ is defined as

$$\mathcal{R}_\epsilon(\mathbf{y}_j) = \sum_n \left(\sqrt{\frac{y_j^2[n]}{\sigma_{\mathbf{y}_j}^2} + \epsilon^2} - \epsilon \right) \quad (12)$$

and $\sigma_{\mathbf{y}_j}^2 = \sum_n y_j^2[n]/N$ is the estimated variance of the deconvolved reflectivity series. As in SMBD the constraint $\mathbf{v}^T \mathbf{v} = 1$ is imposed to avoid a trivial solution. Finally, the deconvolved traces $y_j[n] = d_j[n] * v[n]$ are the per channel estimates of the reflectivity series.

The iterative steepest descent algorithm provides a reliable solution to problems (8) and (11).^{*} The number of parameters in F-SMBD is P , the length of deconvolution filter, while the number in SMBD is JN , so the computational complexity of F-SMBD is significantly lower than SMBD. Furthermore, SMBD and modified SMBD require that regularization parameter(s) in (8) or (10) be chosen which is accomplished with the L-curve or cross validation strategy. Finally, the matrix \mathbf{A} in (6) has $\frac{1}{2}(J-1)JN$ rows, so when the number of traces is large, the memory requirement for SMBD, or modified SMBD, might be too high to store \mathbf{A} for an entire seismic section. Therefore, with hundreds of traces a patch-by-patch strategy would be necessary to manage memory and computation.

3 SMBD via spectral projected-gradient

3.1 Motivation

In existing methods for sparse blind deconvolution, a pseudo ℓ_1 norm regularization of the reflectivity, as in (9) and (12), is used to obtain a least-squares problem. However, with state-of-the-art algorithms it is feasible to attack the ℓ_1 norm optimization directly. The SPG method employed in this paper is based on the general idea of sparsity promoting least squares optimization (for details see [van den Berg and Friedlander, 2008, Hennenfent et al., 2008]). In basis pursuit the ℓ_1 norm is minimized subject to an ℓ_2 constraint

$$\min_{\mathbf{x}} \|\mathbf{x}\|_1 \quad \text{subject to} \quad \|\mathbf{Ax} - \mathbf{b}\|_2 \leq \sigma. \quad (13)$$

For any $\sigma \geq 0$ the basis pursuit problem (also known as basis pursuit denoising (BPDN) if $\sigma > 0$) has an equivalent LASSO problem [Tibshirani, 1996, van den Berg and Friedlander, 2008]

$$\min_{\mathbf{x}} \|\mathbf{Ax} - \mathbf{b}\|_2 \quad \text{subject to} \quad \|\mathbf{x}\|_1 \leq \tau. \quad (14)$$

In other words, after solving (14) for a given τ , the minimum value of $\|\mathbf{Ax} - \mathbf{b}\|_2$ provides the value of σ that would be needed in (13) to get the same \mathbf{x} . The (σ, τ) pairs in this equivalence implicitly define a function $\phi(\tau) = \sigma$, which is convex and differentiable. The graph of $\phi(\tau)$ is the Pareto curve in Figure 2. We

^{*}In eq. (16) of [Nose-Filho et al., 2016] there is a typo for the k -th component of $\nabla \mathcal{L}$, which should be

$$\nabla \mathcal{L}_k = \sum_j \sum_n \frac{\{y_j^2[n]/\sigma_{\mathbf{y}_j}^2 + \epsilon^2\}^{-1/2}}{\sigma_{\mathbf{y}_j}^4} \left\{ \sigma_{\mathbf{y}_j}^2 y_j[n] d_j[n-k] - \frac{y_j^2[n]}{N} \sum_n y_j[n] d_j[n-k] \right\}.$$

want to solve (13), but it is more efficient to solve a sequence of LASSO problems to get the BPDN solution. This requires generating a sequence of $\tau_k \rightarrow \hat{\tau}$, where $\tau_{k+1} = \tau_k + \Delta\tau_k$, for which (14) yields $\{\mathbf{x}_k\}$. For a given $\hat{\sigma}$, the update is based on a straight line extrapolation using the derivative of the Pareto curve: thus, $\Delta\tau_k = (\hat{\sigma} - \phi(\tau_k))/\phi'(\tau_k)$ where $\phi'(\tau_k) = -\|\mathbf{A}^H(\mathbf{A}\mathbf{x}_k - \mathbf{b})\|_\infty/\phi(\tau_k)$.

In seismic data for deconvolution, the reflectivity series of two adjacent channels are typically similar. Using this feature, we can easily estimate the noise level for each channel using its neighboring channels, which serves as a good noise error bound (σ) in the BPDN problem. In addition, this noise level estimate is an average of several channels, which reinforces the lateral continuity in the data. During the SPG method we will (approximately) evaluate $\phi(\tau_k) = \|\mathbf{A}\mathbf{x}_k - \mathbf{b}\|_2$ each time we solve (14) which yields the red dots on the Pareto curve in Figure 2. The convergence rate of this approach is superlinear which is much faster than that of conventional steepest descent gradient methods. Compared with the existing schemes such as SMBD, F-SMBD, and modified SMBD [Kazemi et al., 2016], the primary motivation of our proposed scheme is to provide a much faster numerical approach with a simple way to estimate any parameters that control the algorithm.

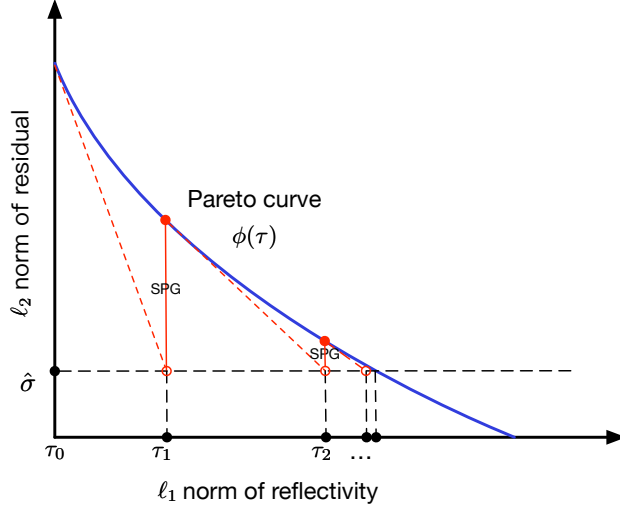


Figure 2: Pareto curve and first three iterations of SPG

3.2 Numerical Scheme

The proposed method, called sparse blind multichannel deconvolution via spectral projected-gradient (SMBD-SPG), is implemented as in Algorithm 1

where

$$\check{\mathbf{d}} = \begin{bmatrix} \mathcal{F}(\mathbf{d}_1) \\ \vdots \\ \mathcal{F}(\mathbf{d}_J) \end{bmatrix}, \quad \mathbf{d} = \begin{bmatrix} \mathbf{d}_1 \\ \vdots \\ \mathbf{d}_J \end{bmatrix} \quad \text{and} \quad \check{\mathbf{R}}^{(k)} = \begin{bmatrix} \text{diag}(\mathcal{F}(\mathbf{r}_1^{(k)})) \\ \vdots \\ \text{diag}(\mathcal{F}(\mathbf{r}_J^{(k)})) \end{bmatrix} \quad (15)$$

and the operator \mathcal{F} is a length- N_{FFT} FFT.

<p>Input: Seismic traces \mathbf{d}_j, for $j = 1, \dots, J$</p> <p>Initialization : Normalize the seismic section according to its global maximal value</p> $\mathbf{d}_j \leftarrow \mathbf{d}_j / \max(\text{abs}(\mathbf{d})) \quad \text{for } j = 1, \dots, J. \quad (16)$ <p>1 Initialize the estimated reflectivity $\mathbf{r}_j^{(0)}$ for each $j \in [1, J]$ using a local peak finder</p> <p>2 for $k \leftarrow 1$ to K do</p> <p>3 Estimate the common wavelet in the frequency domain (check denotes FFT)</p> $\check{\mathbf{w}}^{(k)} = \underset{\check{\mathbf{w}}}{\text{argmin}} \ \check{\mathbf{d}} - \check{\mathbf{R}}^{(k-1)} \check{\mathbf{w}}\ _2^2 + \lambda \ \check{\mathbf{w}}\ _2^2; \quad (17)$ <p>4 $\check{\mathbf{w}}_s^{(k)} = \check{\mathbf{w}}^{(k)} * \mathbf{s}$, where \mathbf{s} is a smoothing filter;</p> <p>5 $\mathbf{w}^{(k)} = \Re\{\text{ifft}(\check{\mathbf{w}}_s^{(k)})\}$;</p> <p>6 Update all J reflectivity series $\mathbf{x} = [\mathbf{r}_1^T, \mathbf{r}_2^T, \dots, \mathbf{r}_J^T]^T$ at once, using SPGL1 to solve:</p> $\mathbf{x}^{(k)} = \underset{\mathbf{x}}{\text{argmin}} \ \mathbf{x}\ _1 \quad \text{subject to } \ \mathbf{d} - \text{diag}\{\mathbf{W}^{(k)}\} \mathbf{x}\ _2 \leq \ \mathbf{z}\ _2, \quad (18)$ <p> where $\mathbf{W}^{(k)}$ is the convolution matrix of $\mathbf{w}^{(k)}$;</p> <p>7 end</p> <p>Output: Estimated source wavelet $\mathbf{w}^{(K)}$ and the J reflectivity series $\mathbf{r}_j^{(K)}$ for $j = 1, \dots, J$</p>
--

Algorithm 1: Sparse blind deconvolution by basis pursuit denoising

For the j -th trace, we need an initial estimate of the reflectivity $\mathbf{r}_j^{(0)}$, so we apply a simple peak locator (**findpeaks** in Matlab) on the received trace \mathbf{d}_j to obtain an initial estimated reflectivity as shown in Figure 3. In order to avoid picking multiple local peaks within the source wavelet itself, we constrain the distance between adjacent peaks to be greater than the wavelet duration. In practice, any efficient peak detector can be employed here to estimate $\mathbf{r}_j^{(0)}$. This initial step only yields a rough estimate of the reflectivity model which is then refined in the following iterative procedure. Although a better initial estimation might lead to faster convergence, the final output is not sensitive to this step as long as we run the algorithm for a sufficient number of iterations.

The assumption of an identical wavelet for all channels is now exploited in the frequency domain. The Fourier transform of the seismic trace \mathbf{d}_j in (2),

$$D_j(e^{j\omega}) = R_j(e^{j\omega})W(e^{j\omega}) + Z_j(e^{j\omega}) \quad (19)$$

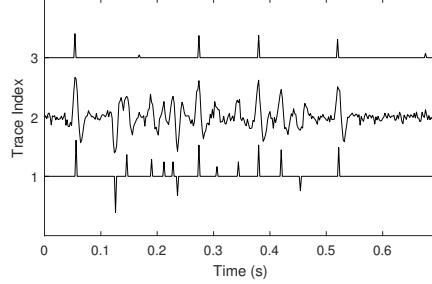


Figure 3: Initial estimated reflectivity using `findpeaks` in Matlab (index = 3) from the original trace (index = 2). The true reflectivity (index = 1) is shown as a reference.

is sampled with an FFT, $\mathcal{F}\{\cdot\}$, to create length- N_{FFT} vectors $\check{\mathbf{d}}_j = \mathcal{F}(\mathbf{d}_j)$, $\check{\mathbf{r}}_j = \mathcal{F}(\mathbf{r}_j)$, and $\check{\mathbf{w}} = \mathcal{F}(\mathbf{w})$. Using the FFTs of the previous estimates of reflectivity in all channels, $\check{\mathbf{r}}_j^{(k-1)} = \mathcal{F}\{\mathbf{r}_j^{(k-1)}\}$, the matrix $\check{\mathbf{R}}^{(k-1)}$ is formed as in (15) and the following minimization problem is solved for the minimum-energy wavelet common to all the channels

$$\check{\mathbf{w}}^{(k)} = \underset{\check{\mathbf{w}}}{\operatorname{argmin}} \|\check{\mathbf{w}}\|_2 \quad \text{subject to } \|\check{\mathbf{d}} - \check{\mathbf{R}}^{(k-1)}\check{\mathbf{w}}\|_2 \leq \|\mathbf{z}\|_2, \quad (20)$$

where $\mathbf{z} = [\mathbf{z}_1^T, \dots, \mathbf{z}_J^T]^T$ is the concatenated noise vector.

By Morozov's discrepancy principle [Morozov, 1984], we can rewrite (20) into a Tikhonov regularization form in (17) for a certain λ , which then has a closed-form solution

$$\check{\mathbf{w}}^{(k)} = (\check{\mathbf{R}}^* \check{\mathbf{R}} + \lambda \mathbf{I})^{-1} \check{\mathbf{R}}^* \check{\mathbf{d}}, \quad (21)$$

where $\check{\mathbf{R}} = \check{\mathbf{R}}^{(k-1)}$ for conciseness. The diagonal-blocks structure of $\check{\mathbf{R}}$ implies that $\check{\mathbf{R}}^* \check{\mathbf{R}}$ is diagonal, which eliminates the need to compute a matrix inverse in (21).

In practice, a seismic source typically has a smooth band-limited spectrum, but adding a regularization term to reflect the smoothness of the spectra is difficult, so we apply a smoothing filter after solving (17) with (21). Frequency domain smoothing applied to $\check{\mathbf{w}}^{(k)}$ is equivalent to windowing in the time domain near zero (see Figures 6b and 6d).

Given the estimated wavelet $\mathbf{w}^{(k)}$, the updated reflectivity $\mathbf{r}_j^{(k)}$ is obtained by deconvolving the wavelet with basis pursuit. To obtain a sparse result for the reflectivity sequences, we solve the following BPDN problem *for all channels* at once:

$$\mathbf{x}^{(k)} = \underset{\mathbf{x}}{\operatorname{argmin}} \|\mathbf{x}\|_1 \quad \text{subject to } \|\mathbf{d} - \operatorname{diag}\{\mathbf{W}^{(k)}\}\mathbf{x}\|_2 \leq \|\mathbf{z}\|_2, \quad (22)$$

where $\mathbf{W}^{(k)}$ is the convolution matrix of $\mathbf{w}^{(k)}$. For fast numerical implementation, instead of generating the large diagonal matrix with J copies of $\mathbf{W}^{(k)}$ and computing the matrix multiplication directly, it is more efficient to calculate the

individual convolutions $\mathbf{W}^{(k)} \mathbf{r}_j^{(k)}$. As an aside, we note that including the Euclid deconvolution term $\|\mathbf{A}\mathbf{x}\|_2$ in this problem would destroy the computational simplicity of the algorithm that solves BPDN.

4 Parameter choices

In SMBD-SPG several parameters require attention. First, in a least squares problem $\mathbf{A}\mathbf{x} + \mathbf{n} = \mathbf{b}$, where \mathbf{n} is a noise vector and \mathbf{b} the vector of observations, the solution to the Tikhonov regularization problem

$$\min_{\mathbf{x}} \|\mathbf{A}\mathbf{x} - \mathbf{b}\|_2^2 + \lambda \|\mathbf{x}\|_2^2 \quad (23)$$

has a closed-form

$$\mathbf{x}_\lambda = (\mathbf{A}^T \mathbf{A} + \lambda \mathbf{I})^{-1} \mathbf{A}^T \mathbf{b}. \quad (24)$$

If $\|\mathbf{n}\|_2 \leq \delta$ and $\mathbf{A}^T \mathbf{b} \in \text{Range}(\mathbf{A}^T \mathbf{A})$, we have

$$\|\mathbf{x}_\lambda - \mathbf{A}^T \mathbf{b}\|_2 \leq \delta / \sqrt{\lambda} + O(\lambda), \quad (25)$$

so $\lambda = C\delta^{2/3}$ is a asymptotic “brick wall” for Tikhonov regularization [Groetsch, 2010]. For (17), if the noise level $\|\mathbf{z}\|_2$ can be estimated, we can pick $\lambda = C(\|\mathbf{z}\|_2)^{2/3}$ which is optimal in the asymptotic sense.

Next, the noise levels $\|\mathbf{z}\|_2 = (\sum_j \|\mathbf{z}_j\|_2^2)^{1/2}$ must be chosen for (18). Here we need estimates of the noise energy on the traces, for $j = 1, \dots, J$. If we assume the noise is spatially stationary then the noise energy has roughly the same level on neighboring channels. Because the reflectivity is determined by the real earth, as well as the relative locations of the sensors and the seismic source, a high degree of resemblance for the reflectivity in spatially close channels is commonly observed [Aki and Richards, 2009]. Under these assumptions, we can calculate the variance of the difference of two adjacent traces to estimate the incoherent noise energy

$$\begin{aligned} \text{Var}(\mathbf{d}_1 - \mathbf{d}_2) &= \text{Var}(r_1[n] * w[n] + z_1[n] - r_2[n] * w[n] + z_2[n]) \\ &\approx \text{Var}(z_1[n] - z_2[n]) = 2\text{Var}(z[n]) \end{aligned} \quad (26)$$

which then leads to $\|\mathbf{z}_j\|_2 \approx \sqrt{N\text{Var}(z_j[n])}$. For the high SNR case, where a silent segment (noise only part) of traces can be easily identified, we can use the silent segments to replace the whole traces \mathbf{d}_1 and \mathbf{d}_2 in (26) for better estimation.

Finally, the wavelet length could be estimated based on the knowledge of the equipment used in the seismic survey. In the examples presented here, however, we adopt a wavelet length of 51 sample points for SMBD-SPG.

5 Synthetic data test

In the synthetic test we generate 20 traces using the reflectivity shown in Figure 1b, which can be downloaded at [Liu et al., 2016], where the sampling

frequency is 500 Hz. Throughout this paper, all experiments were performed on Matlab R2016b with a 3.5 GHz Intel i7 quad-core CPU and 32 GB RAM. The received data in Figure 1c is the convolution of the reflectivity with a Ricker wavelet of center frequency 40 Hz with 50 degrees of phase shift (in Figure 1a) plus additive white Gaussian noise (AWGN) of SNR = 10 dB. The SNR adopted in this work for the signal-plus-noise model $\mathbf{x} = \mathbf{s} + \mathbf{n}$ is defined as

$$\text{SNR} = 10 \log_{10} \left(\frac{\|\mathbf{s}\|_2^2}{\|\mathbf{n}\|_2^2} \right), \quad (27)$$

where $\|\mathbf{s}\|_2^2$ is the total signal energy and $\|\mathbf{n}\|_2^2$ the noise energy.

For the F-SMBD algorithm, a length-51 deconvolution filter is used, which is initialized with a single spike located at the middle of the filter. Other parameters used for F-SMBD are $\epsilon = 1$, and step size $\mu = 0.02$. For the SMBD algorithm, the regularization parameter λ is set to 4, the smoothed norm parameter ϵ is set to 0.0001, and $\alpha = 0.2$. The number of iterations for SMBD and F-SMBD are set to 800 and 500, respectively, which ensures that both algorithms converge.

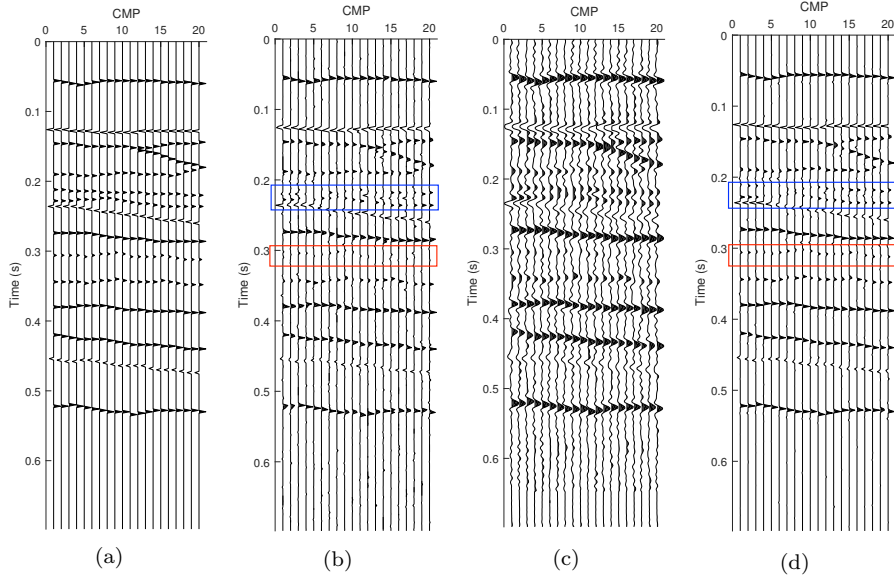


Figure 4: Deconvolution result for SNR = 10 dB. (a) True reflectivity. Deconvolution result for (b) SMBD, (c) F-SMBD, (d) SMBD-SPG (5 iterations).

The recovered reflectivity series using the three methods are shown in Figure 4b,c,d. For SMBD-SPG the number of iterations is set equal to 5, i.e., $K = 5$ in Algorithm 1. Overall, SMBD-SPG gives results comparable to SMBD, or slightly better. Within the blue and red rectangles, we notice that SMBD-SPG is slightly better for weak and close reflectors, in the sense that information

with better precision is preserved for interpretation. The quality of the three methods is evaluated using the normalized power spectrum density (PSD) as well, shown in Figure 5. SMBD-SPG yields the flattest PSD among the three schemes, which is closest to the PSD of the true reflectivity. SMBD is nearly as flat in the frequency domain, while F-SMBD exhibits an obvious band limit to frequencies below 80 Hz.

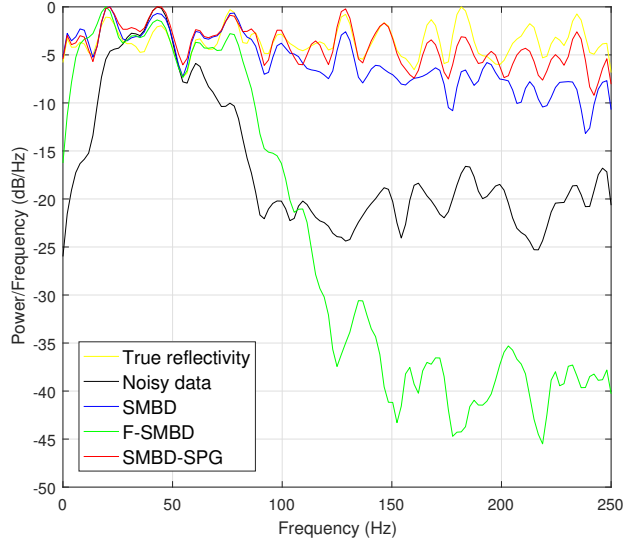


Figure 5: Smoothed normalized PSD of the true reflectivity, noisy data and recovered reflectivity series. SNR = 10 dB, SMBD-SPG with 5 iterations. PSD computed per channel via MATLAB’s `pwelch` function with section length = 100 and overlap = 60, and then averaged over all channels.

Although the SMBD-SPG scheme is an iterative algorithm, in many cases only a few iterations are needed to get a good approximation of the wavelet due to the smoothing filter. For example, the result in Figure 4d is obtained after only 5 iterations. The estimated wavelet with and without smoothing in frequency and windowing in time can be found in Figure 6. Note the accurate match after applying the smoothing filter in Figure 6b, where the smoothing filter is of length-11 with uniform values. After getting the time-domain wavelet, a portion of it is taken (which consists of 51 samples and indicated as a rectangle in Figure 6d) to be used for updating the reflectivity in (18). In Figure 7 we show the estimated wavelet’s spectrum before and after smoothing after 1 and 3 iterations, so we can observe the amount of improvement over iterations.

To compare the performance of SMBD-SPG with SMBD and F-SMBD, two quality metrics are used to measure the similarity between the reflectivity \mathbf{x} and its estimate $\hat{\mathbf{x}}$. The normalized correlation coefficient γ and the quality Q are

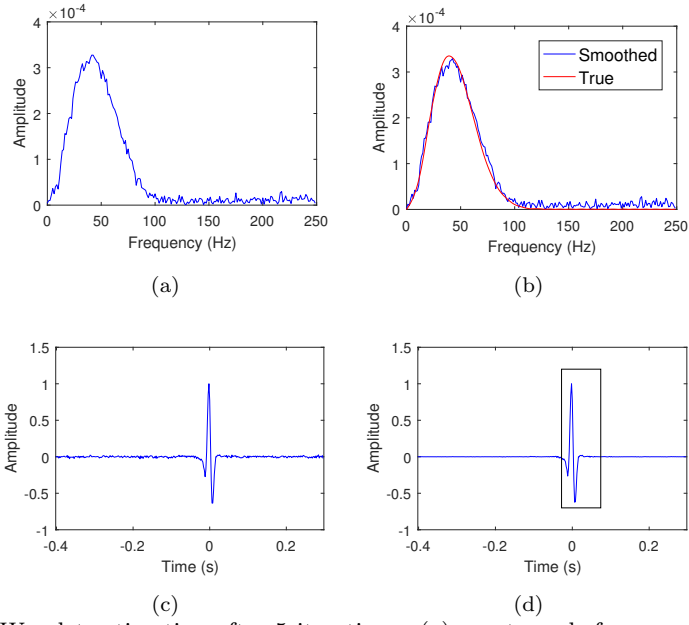


Figure 6: Wavelet estimation after 5 iterations. (a) spectrum before smoothing, (b) smoothed and true spectrum, (c) time-domain wavelet before smoothing, (d) wavelet after smoothing.

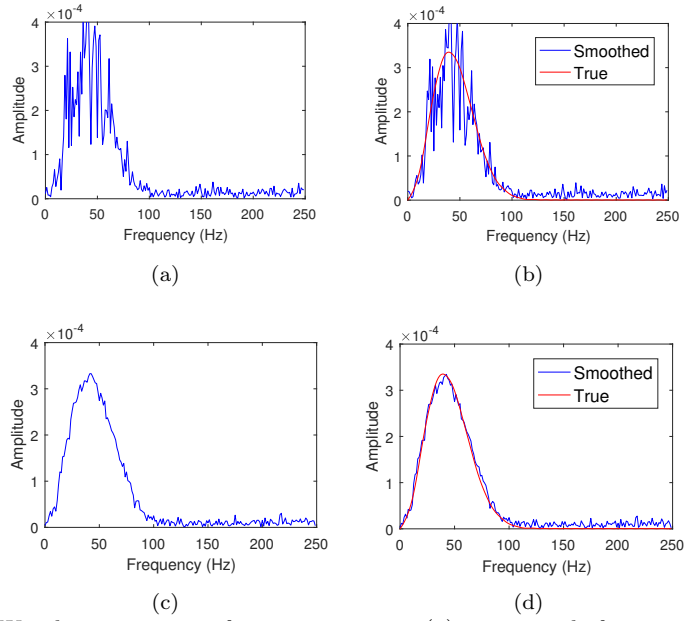


Figure 7: Wavelet estimation after one iteration: (a) spectrum before smoothing, (b) smoothed and true spectrum. Wavelet estimation after three iterations: (c) spectrum before smoothing, (d) smoothed and true spectrum.

defined by

$$\gamma = \frac{\hat{\mathbf{x}}^T \mathbf{x}}{\sqrt{(\hat{\mathbf{x}}^T \hat{\mathbf{x}})(\mathbf{x}^T \mathbf{x})}} \quad (28a)$$

$$Q = 20 \log_{10} \frac{\|\mathbf{x}/(\mathbf{x}^T \mathbf{x})\|_2}{\|\mathbf{x}/(\mathbf{x}^T \mathbf{x}) - \hat{\mathbf{x}}/(\hat{\mathbf{x}}^T \hat{\mathbf{x}})\|_2}, \quad (28b)$$

where \mathbf{x} and $\hat{\mathbf{x}}$ are long vectors formed by concatenating true and estimated reflectivity series, respectively. After running 10 Monte-Carlo realizations of the random noise for various levels, the mean value and standard deviation are shown in Figures 8c and 8d for γ and Q versus SNR. As can be seen from these figures, the SMBD-SPG algorithm (after 5 iterations) outperforms the SMBD and F-SMBD algorithms in terms of γ and Q for all noise levels.

To show that the proposed algorithm is faster than SMBD and F-SMBD, calculation time taken by the algorithms is plotted against the number of traces (each trace contains 350 time samples) in Figure 8b. We can see that SMBD-SPG takes much even less time than F-SMBD. Specifically, the computation time of 5 iterations of SMBD-SPG for 60 traces equals 0.1773 s, which is 0.0926% of the SMBD time and 2.38% of F-SMBD.

6 Real data results

In this section, results obtained using SMBD, F-SMBD and SMBD-SPG on a real seismic data set are presented. The seismic data is from the National Petroleum Reserve, Alaska (NPRA) Legacy Data Archive by USGS (1976), Line ID 31-81 [NPRA, 1976].

For the real data scenario, we run SMBD on blocks of duration 0.6 s in time and 100 traces. For F-SMBD, the deconvolution filter length is taken as 51 samples with a spike at the middle of the filter for initialization. The learning rate for F-SMBD is set to $\mu = 0.02$. The deconvolution filter for F-SMBD is obtained for part of the data, i.e., time range [0.6, 2.4], and traces 251 to 254. For SMBD-SPG, the blocks are the same as in SMBD. The remaining parameters of all three algorithms are unchanged from the synthetic data test. The average processing times for each patch are 95.22 s and 0.7618 s for SMBD and SMBD-SPG, respectively. Recently, the authors of SMBD proposed a modified SMBD [Kazemi et al., 2016] method by adopting an iterative scheme that alternates between wavelet estimation and reflectivity estimation. It turns out the performances have been greatly improved, however each iteration of the modified SMBD requires similar computational efforts to SMBD. In this paper, our aim is to provide an alternative quick solution which has the same level of performance if not better than the popular multi channel blind deconvolution methods. Thus, we do not compare our results to the modified SMBD here.

Figure 9 shows the input data and the deconvolution results for all three algorithms. The details of a zoomed-in seismic section before and after deconvolution are shown in Figure 10. It is clear from these results that the proposed

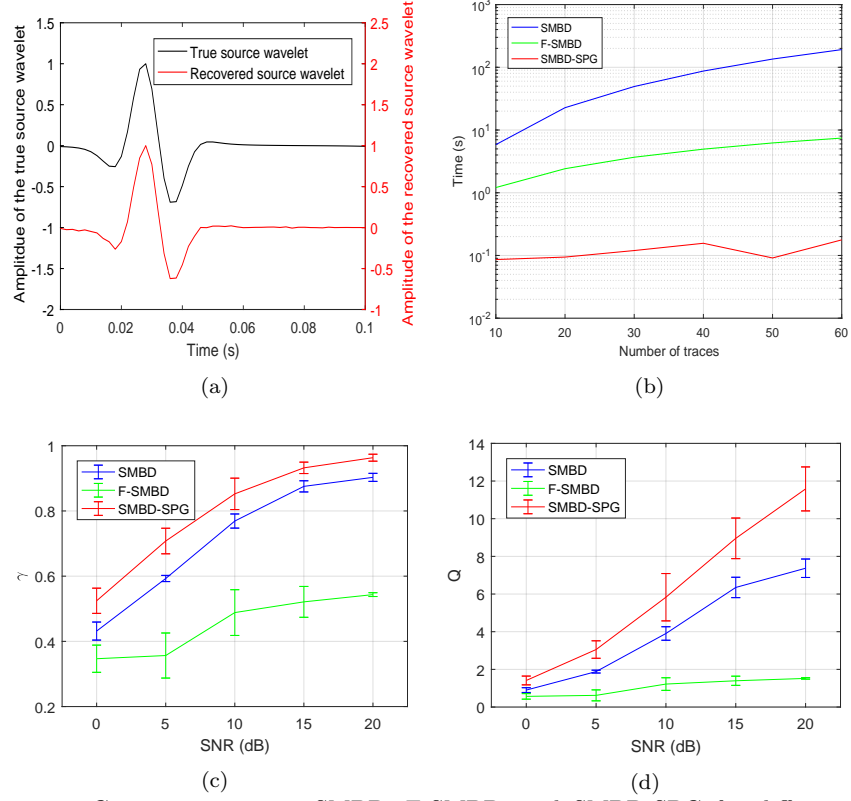


Figure 8: Comparison among SMBD, F-SMBD, and SMBD-SPG for different attributes of the synthetic data example. (a) Recovered wavelet (by SMBD-SPG) and true wavelet with SNR = 10 dB; (b) Simulation time vs. number of traces with SNR = 10 dB, each trace contains 350 samples; (c) Normalized correlation coefficient γ vs. SNR (mean and standard deviation averaged over 20 traces); (d) Quality metric Q vs. SNR (mean and standard deviation over 20 traces).

algorithm has a more spiky deconvolution output and more weak reflections are preserved than the other two algorithms. In Figure 11 we show three processing blocks in blue rectangles and their corresponding recovered source wavelets, where the consistency and quality of the estimates is easy to observe.

7 Conclusions

In the multichannel blind deconvolution problem, the assumption of an identical seismic source wavelet in all channels leads naturally to a two-step algorithm that alternately estimates the wavelet given the reflectivity and then updates the reflectivity given the wavelet. Previous multichannel blind deconvolution methods have used the identical wavelet assumption to obtain the Euclid

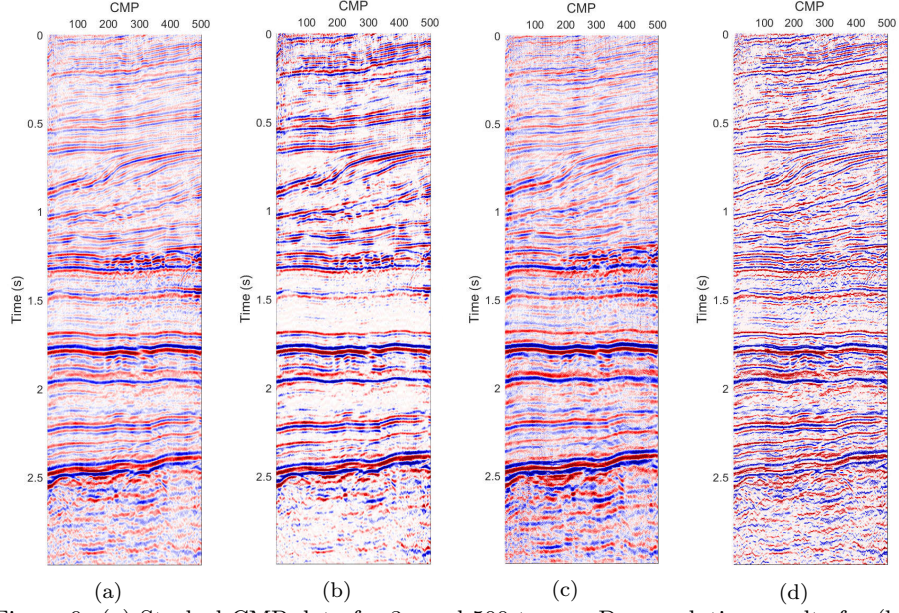


Figure 9: (a) Stacked CMP data for 3s and 500 traces. Deconvolution results for (b) SMBD, (c) F-SMBD, (d) SMBD-SPG (5 iterations).

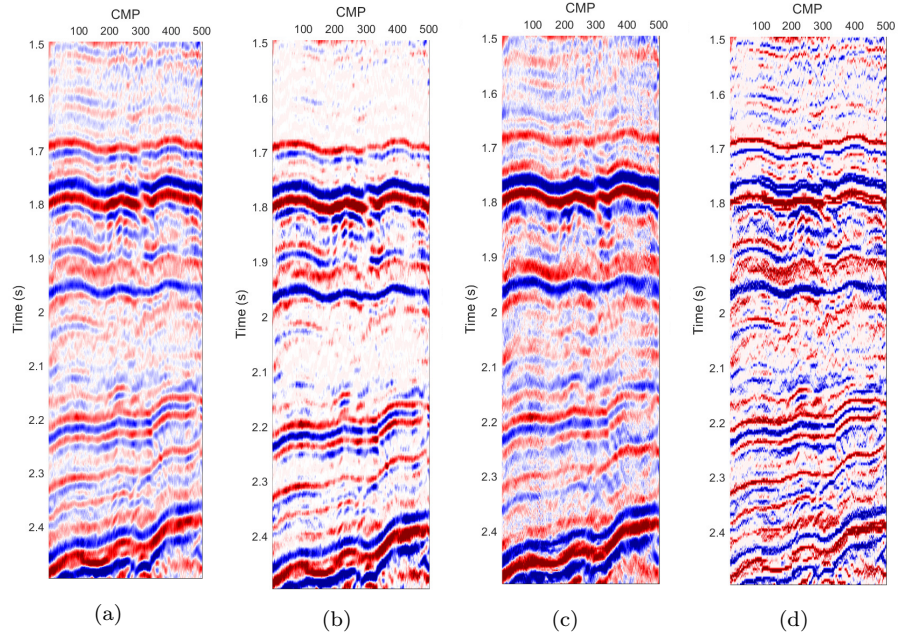


Figure 10: (a) Subset of the stacked CMP data for $1.5 \leq t \leq 2.5$ s and 500 traces. Deconvolution results for (b) SMBD, (c) F-SMBD, (d) SMBD-SPG (5 iterations).

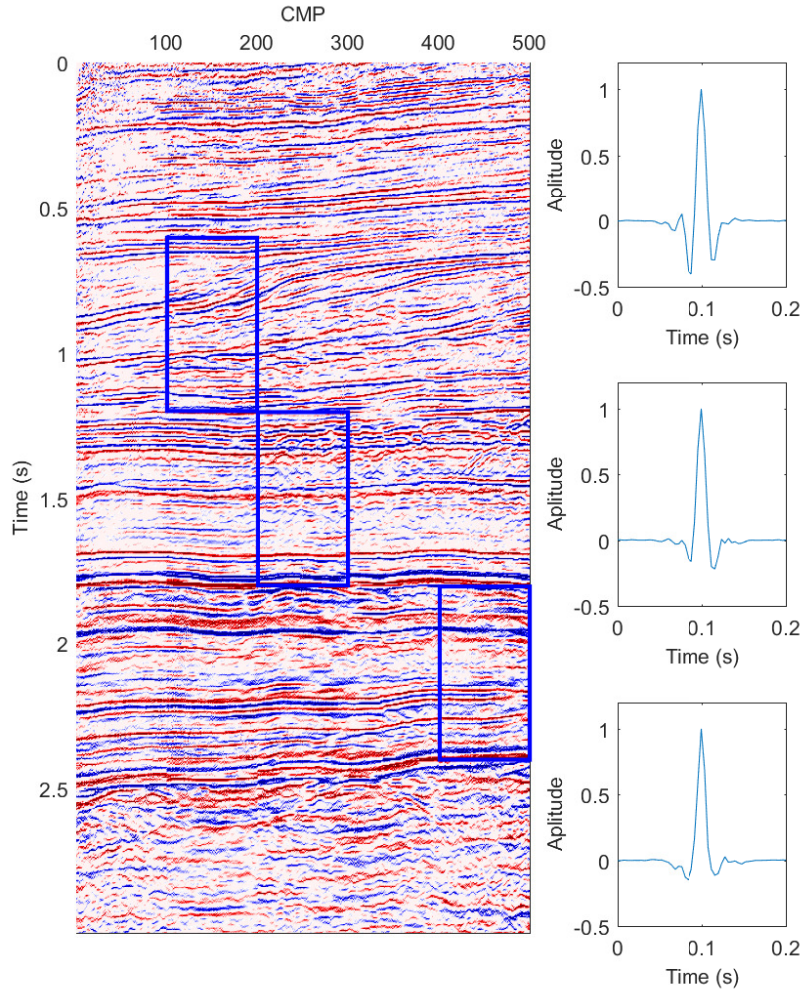


Figure 11: Recovered wavelet for SMBD-SPG in three distinct processing blocks.

deconvolution property (5) which eliminates the wavelet. However, we use all the channels at once to recover the wavelet in the frequency domain which effectively increases the SNR of the recovered wavelet. For the reflectivity update we exploit sparsity in order to express the reflectivity update as basis pursuit denoising. The reflectivity estimate is updated for *all channels* via sparse recovery with BPDN, which can be efficiently solved using the SGPL1 package—one of the best available fast ℓ_1 methods. This approach ensures the computational efficiency of SMBD-SPG. Also, in SMBD-SPG only two parameters must be set, which makes the scheme easy to implement for real applications. As a final comment, we note that the Euclid deconvolution property leads to a term $\|\mathbf{Ax}\|_2$ in the SMBD objective functionals, (8) and (10), which cannot be incorporated into the BPDN framework and its efficient algorithmic solution.

In the simulation with synthetic data, the quality of the recovery is evaluated versus the known true reflectivity. The SMBD-SPG method is robust to noise, i.e., it provides results slightly better than SMBD and much better than F-SMBD with respect to the metrics of normalized correlation and quality for a wide range of SNR. In addition, to achieve the same or better quality deconvolution outputs, the computation time for SMBD-SPG is significantly less than either F-SMBD or SMBD (more than two orders of magnitude faster in some cases in Figure 8b).

Acknowledgement

This work is supported by the Center for Energy and Geo Processing (CeGP) at Georgia Tech. We also appreciate the support provided by the CeGP at King Fahd University of Petroleum and Minerals (KFUPM) under project number GTEC1311.

References

- [Aki and Richards, 2009] Aki, K., and P. G. Richards, 2009, Quantitative seismology, 2nd ed.: University Science Books.
- [Behm and Shekar, 2014] Behm, M., and B. Shekar, 2014, Blind deconvolution of multichannel recordings by linearized inversion in the spectral domain: Geophysics, **79**, V33–V45.
- [Bostock, 2004] Bostock, M. G., 2004, Green’s functions, source signatures, and the normalization of teleseismic wave fields: Journal of Geophysical Research: Solid Earth, **109**, B03303.
- [Bostock and Sacchi, 1997] Bostock, M. G., and M. D. Sacchi, 1997, Deconvolution of teleseismic recordings for mantle structure: Geophysical Journal International, **129**, 143–152.

- [Gholami and Sacchi, 2012] Gholami, A., and M. Sacchi, 2012, A fast and automatic sparse deconvolution in the presence of outliers: *IEEE Transactions on Geoscience and Remote Sensing*, **50**, 4105–4116.
- [Groetsch, 2010] Groetsch, C., 2010, Linear inverse problems, *in Handbook of Mathematical Methods in Imaging*: Springer, 4–41.
- [Hennenfent et al., 2008] Hennenfent, G., E. van den Berg, M. P. Friedlander, and F. J. Herrmann, 2008, New insights into one-norm solvers from the Pareto curve: *Geophysics*, **73**, A23–A26.
- [Herrera and van der Bann, 2012] Herrera, R. H., and M. van der Bann, 2012, Short-time homomorphic wavelet estimation: *Journal of Geophysics and Engineering*, **9**, 674–680.
- [Kaaresen and Taxt, 1998] Kaaresen, K. F., and T. Taxt, 1998, Multichannel blind deconvolution of seismic signals: *Geophysics*, **63**, 2093–2107.
- [Kazemi et al., 2016] Kazemi, N., A. Gholami, and M. D. Sacchi, 2016, Modified sparse multichannel blind deconvolution: Presented at the 78th EAGE conference & Exhibition, EAGE.
- [Kazemi and Sacchi, 2014] Kazemi, N., and M. Sacchi, 2014, Sparse multichannel blind deconvolution: *Geophysics*, **79**, V143–V152.
- [Liu et al., 2016] Liu, E., N. Iqbal, J. H. McClellan, and A. Al-Shuhail, 2016, A synthetic reflectivity model: http://cegp.ece.gatech.edu/assets/syn_model.mat/.
- [Morozov, 1984] Morozov, V. A., 1984, *Methods for solving incorrectly posed problems*: Springer-Verlag.
- [Nose-Filho et al., 2016] Nose-Filho, K., A. K. Takahata, R. Lopes, and J. M. Romano, 2016, A fast algorithm for sparse multichannel blind deconvolution: *Geophysics*, **81**, V7–V16.
- [NPRA, 1976] NPRA, 1976, USGS CMG N-PR-76-AK Metadata: <https://walrus.wr.usgs.gov/namss/survey/n-pr-76-ak/>.
- [Otis and Smith, 1977] Otis, R., and R. Smith, 1977, Homomorphic deconvolution by log spectral averaging: *Geophysics*, **42**, 1146–1157.
- [Ram et al., 2010] Ram, I., I. Cohen, and S. Raz, 2010, Multichannel deconvolution of seismic signals using statistical MCMC methods: *IEEE Transactions on Signal Processing*, **58**, 2757–2770.
- [Rietsch, 1997] Rietsch, E., 1997, Euclid and the art of wavelet estimation, Part I: Basic algorithm for noise-free data: *Geophysics*, **62**, 1931–1938.
- [Robinson and Treitel, 1980] Robinson, E. A., and S. Treitel, 1980, *Geophysical signal analysis*: Prentice Hall, Inc.
- [Tibshirani, 1996] Tibshirani, R., 1996, Regression shrinkage and selection via the lasso: *J. Roy. Statist. Soc. Ser. B.*, 267–288.

- [Tria et al., 2007] Tria, M., M. van der Baan, A. Larue, and J. W. Mars, 2007, Wavelet estimation and blind deconvolution of realistic synthetic seismic data by log spectral averaging: 77th Annual International Meeting, SEG, Expanded Abstracts, SEG, 1982–1986.
- [Ulrych et al., 1995] Ulrych, T., D. Velis, and M. D. Sacchi, 1995, Wavelet estimation revisited: The Leading Edge, **14**, 1139–11143.
- [van den Berg and Friedlander, 2008] van den Berg, E., and M. P. Friedlander, 2008, Probing the Pareto frontier for basis pursuit solutions: SIAM Journal on Scientific Computing, **31**, 890–912.
- [van der Bann and Pham, 2008] van der Bann, M., and D.-T. Pham, 2008, Robust wavelet estimation and blind deconvolution of noisy surface seismic: Geophysics, **73**, V37–V46.
- [Wiggins, 1978] Wiggins, R. A., 1978, Minimum entropy deconvolution: Geoprospection, **16**, 21–35.
- [Xu et al., 1995] Xu, G., H. Liu, L. Tong, and T. Kailath, 1995, A least-squares approach to blind channel identification: IEEE Transactions on Signal Processing, **43**, 2982–2993.
- [Yilmaz, 2001] Yilmaz, O., 2001, Seismic data analysis: Processing, inversion and interpretation of seismic data, 2nd ed.: SEG.